Nuclear-magnetic-resonance studies of strain in isovalently doped GaAs

W. E. Carlos and S. G. Bishop*
Naval Research Laboratory, Washington, D.C. 20375

D. J. Treacy
U.S. Naval Academy, Annapolis, Maryland 21402
(Received 26 October 1990)

The deviations from tetrahedral symmetry induced by indium substituting for gallium in GaAs are probed by using nuclear magnetic resonance (NMR) to study the first- and second-order nuclear quadrupole interactions of the arsenic and indium atoms. The indium atoms are found to be randomly distributed on the gallium sublattice. The strain field is sufficient to affect the NMR of either the In or the As nuclei at distances of about 30 Å from an In atom. Second-order nuclear quadrupole interactions in the As NMR are used to determine specific bond-angle distortions for the first shells of atoms around an In atom.

I. INTRODUCTION

Isovalent impurities in III-V semiconductors have attracted considerable research interest in recent years because of lattice hardening effects which result from their incorporation at relatively high concentrations. For example, the introduction of indium impurities in GaAs at concentrations up to 10^{20} cm^{-3} has produced dramatic reductions in dislocation density without significant loss of semi-insulating properties.[1-3] In order to understand the mechanism(s) for the reduction of the dislocation density and to assess possible effects on the transport properties of the material, it is important to achieve a detailed understanding of the incorporation of the isovalent impurities in the zinc-blende crystal lattice. It is particularly important to characterize the stress or distortion induced in the lattice by the presence of isovalent impurities. Because of their isovalent character, these impurities are not electrically active as dopants, they are not paramagnetic, and they are not usually optically active. The traditional transport measurements such as the Hall effect yield little or no information concerning the isovalent impurities, and various spectroscopic techniques such as electron paramagnetic resonance (EPR) and photoluminescence (PL) cannot directly probe these isoelectronic centers.

We have used nuclear-magnetic-resonance (NMR) spectroscopy to probe the local structural environment of isovalent impurities in GaAs. The isovalent (neutral) character of the impurities assures that the nuclear electric quadrupole interaction, which senses electric field gradients at the nuclear sites, will be determined primarily by atomic displacements or bond-angle distortions induced in the tetrahedral lattice by the presence of the impurity atoms rather than by interactions with large concentrations of charged impurities. For example, ^{115}In, ^{75}As, and ^{69}Ga NMR spectra have been used to characterize bond-angle distortions in the first few coordination spheres surrounding the In atoms in GaAs:In and to determine the longer-range spatial extent of the strain introduced by the isovalent impurity atoms.

The structural information derived from these NMR studies of dilute alloys complements the results of the extended x-ray absorption fine structure (EXAFS) studies of the more concentrated $Ga_{1-x}In_xAs$ alloys carried out by Mikkelsen and Boyce.[4] Their seminal work showed that the GaAs and the InAs bond lengths vary by less than 2% across the alloy system and provided measurements of the next-nearest-neighbor separations (Ga-Ga, Ga-In, In-In, and As-As). The cation-cation separations for various compositions of the alloy were found to approximate the distances expected under the virtual crystal approximation (VCA) while the anion-anion (As-As) separations had a bimodal distribution around the values for the GaAs and InAs lattices. The NMR measurements are found to be consistent with several of the principal EXAFS results including the measured values of next-nearest-neighbor distances and the observation that most of the distortion which occurs in this lattice mismatched alloy is accommodated in the common or pure (anion) As sublattice.

II. APPLICATION OF NMR TO SEMICONDUCTORS

Nuclear-magnetic-resonance spectroscopy can provide valuable information concerning short-range (primarily near neighbors) structural configurations in solids. The dipole-dipole, electric quadrupole, and chemical shift interactions can shift, split, or broaden the NMR spectrum, and it is these interactions of the resonant nuclei with neighboring nuclear magnetic moments, ions, or bonding electrons which serve as local probes of the nuclear environment. For example, the chemical shift arises because of paramagnetic and diamagnetic interactions between electrons around a nucleus and the applied magnetic field which produce an additional local magnetic field at the nuclear site. In its simplest manifestation the chemical shift can be treated as a scalar whose magnitude provides

a measure of the relative ionicity of the chemical bonds which involve the resonant nuclei.

Recently, Akimoto, Mori, and Kojima have studied ^{27}Al chemical shifts in $Al_xGa_{1-x}As$ and have inferred that the Al—As bond strength decreases with increasing aluminium content x.[5] It is also possible to distinguish different bonding configurations on the basis of their chemical shifts. Beshah *et al.* have shown that various structural units can be distinguished from each other in $Hg_xCd_{1-x}Te$ alloys and have suggested on the basis of their NMR measurements that the relative concentrations of these structural units depart from the values expected for a random alloy.[6]

In contrast, the quadrupolar interaction, which involves the interaction of the nuclear electric quadrupole moment with electric field gradients (EFG's) at the nuclear site, can distinguish different bonding configurations only on the basis of different symmetries. For example, in an alloy with tetrahedral bonding, $A_xB_{1-x}C$, the quadrupolar interaction readily distinguishes between A_4C and A_3BC configurations, but not between A_4C and B_4C configurations. However, of overriding importance to the present work is the fact that quadrupolar interaction is extremely sensitive to small deviations from symmetry (bond-angle distortions on the order of 0.01°) and therefore can be used for quantitative measurements of bond-angle distortions.

Early studies of binary III-V semiconductors by cw NMR spectroscopy[7] and nuclear acoustic resonance (NAR) techniques[8] established the roles of the dipolar interaction, the indirect exchange interaction between unlike spins, the pseudodipolar interaction, and the quadrupole interaction in determining the second moments of the NMR lines in these zinc-blende structure crystals. More recently, Cueman *et al.*[9] have used pulsed NMR to detect the effects of very small concentrations of charged defects on the second moment of the NMR lines in GaAs. All of these studies utilized crystals in which the perturbations of the NMR were relatively small, and manifested themselves as changes in the second moment of a single resonance line. The second moments of the resonance lines reported in (7) and (9) for the ^{75}As resonance were of the order of 1–10 G.[2] This range of second moments is consistent with those reported using NAR.[8]

A more direct antecedent of the present investigation is the work of Rhoderick, who observed the effects of large concentrations of substitutional impurities on cw NMR line intensities in III-V compounds.[10] Rhoderick's studies involved the doping of InSb and GaAs with either charged or isovalent (neutral) impurities at concentrations ranging up to 10^{20} cm^{-3}. He found that the EFG's induced at the nuclear sites surrounding both charged and isovalent impurities produced quadrupole interactions which removed intensity from the NMR lines. This intensity loss increased with increasing impurity concentration and it was determined that the concentrations of charged impurities on the order of 10^{19} cm^{-3} were sufficient to affect the In resonance for every In atom in a sample of InsB. Correspondingly, the concentration of isovalent impurities required to cause a comparable intensity decrease in InSb was of the order of 30 times higher.

Rhoderick also performed experiments using the ^{69}Ga NMR in In-doped GaAs which closely parallel the work discussed here. In this system he found that the distortions introduced in the crystal lattice by isovalent In impurity concentrations of the order of 10^{20} cm^{-3} were sufficient to affect the NMR of every Ga atom in a sample of GaAs. Specifically, the impurity-induced distortions produce first-order quadrupole interactions which are of sufficient magnitude to split out the $m=\pm\frac{3}{2}$ to $\pm\frac{1}{2}$ satellite transitions at every site. From these results he inferred a sphere of influence or strain radius surrounding an isolated In impurity in the GaAs lattice. Rhoderick's and other previous studies were subject to several limitations which are much less severe in the present work. In this work very high-quality semi-insulating single crystals were used, while in previous work less pure, and in some cases powdered samples, were studied. In the current work much higher magnetic fields which increase signal-to-noise ratio and permit observation of second-order effects are used. The pulse techniques used in these experiments also increase sensitivity and allow emphasis of particular transitions. Thus it has been possible to investigate the orientation dependence of features in the NMR line shape and to detect the satellite transitions which have been shifted out from the central resonance by the quadrupole interaction.[11] The increased sensitivity also allows us to observe the NMR of impurity atoms and to resolve features attributable to a single shell of atoms around that impurity atom.

III. THE NUCLEAR ELECTRIC QUADRUPOLE INTERACTION

The Zeeman interaction between the magnetic dipole moment of a nucleus with spin I and an applied static magnetic field H produces a series of $2I+1$ equally spaced quantized energy levels with multiplicity determined by $m=I,I-1,\ldots,-I$. Resonant transitions between these levels governed by the selection rule $\delta m=\pm 1$ result in an absorption line at the Larmor frequency given by

$$2\pi\nu_0=\gamma H \ . \tag{1}$$

Nuclei having spin greater than $\frac{1}{2}$ (this includes all group-III and group-V elements except P) have an electric quadrupole moment which will couple to an EFG at the nuclear site. This quadrupole interaction causes shifts in the NMR spectrum which can provide valuable information concerning the local bonding configuration. At an unperturbed lattice site the EFG will be zero and there will be no quadrupole interaction. In the experiments described here the interaction of the nuclear electric quadrupole moment Q with the EFG is used to probe lattice distortions introduced by isovalent impurities. Because of the difference between the In—As or Ga—Sb bond lengths and the Ga—As bond lengths of the host lattice, the lattice sites in the vicinity of the impurity atoms in In- or Sb-doped GaAs will deviate from perfect symmetry and have a nonzero EFG.

The matrix describing the interaction between the EFG and the nuclear electric quadrupole moment may be diagonalized and has a trace of zero. The z axis is taken to be the direction of maximum field gradient and the x axis the direction of minimum field gradient. The two parameters characterizing the quadrupole interaction are the quadrupole coupling constant, ν_Q and the asymmetry parameter[12] η, which are given by

$$\nu_Q = 3eV_{zz}Q/2I(2I-1)h \ , \tag{2a}$$

$$\eta = (V_{yy}-V_{xx})/V_{zz} \ , \tag{2b}$$

where the V_{ii} are the components of the EFG tensor. For a site having an n-fold rotation axis or a rotation-reflection axis with $n>2$, $\eta=0$ and, as noted above, at high-symmetry sites such as those having tetrahedral symmetry, $V_{zz}=0$.

In the work reported here the quadrupolar interactions are much weaker than the Zeeman interaction and therefore a simple perturbation expansion may be used to describe them. Slight deviations from tetrahedral symmetry are well described by first-order terms which split the satellite transitions (e.g., $m=+\frac{3}{2}$ to $+\frac{1}{2}$) out of the central resonance, while larger deviations produce noticeable second-order effects which shift the central resonance. The first- and second-order frequency shifts are

$$\delta\nu^{(1)} = -\tfrac{1}{2}(m-\tfrac{1}{2})\nu_Q(3\cos^2\theta - 1 - \eta\sin^2\theta\cos 2\phi) \ , \tag{3}$$

$$\delta\nu^{(2)} = (\nu_Q^2/12\nu_0)\{\tfrac{3}{2}\sin^2\theta[(\alpha+\beta)\cos^2\theta-\beta] + \eta\cos 2\phi\sin^2\theta[(\alpha+\beta)\cos^2\theta+\beta] + \eta^2/6[\alpha-(\alpha+4\beta)\cos^2\theta-(\alpha+\beta)\cos^2 2\phi\sin^4\theta]\} \tag{4}$$

where

$$\alpha = 24m(m-1)-4I(I+1)+9$$

and

$$\beta = \tfrac{1}{4}[6m(m-1)-2I(I+1)+3] \ .$$

Note that by varying the resonant frequency ν_0, we can readily distinguish between chemical shifts (proportional to ν_0), first-order quadrupolar effects (independent of ν_0), and second-order quadrupolar effects (inversely proportional to ν_0).

IV. EXPERIMENTAL PROCEDURES

A. Samples

The experiments described here were performed on semi-insulating crystals of GaAs which were grown by the liquid encapsulated Czochralski (LEC) technique. The samples and some of their properties are listed in Table I. Sample Nos. 1–4, 6, and 7 were provided by the Air Force Wright-Patterson Materials Research Laboratory (AFWMRL) and sample No. 5 is a sample from Westinghouse Research Center. The growth techniques employed routinely produce crystals with extremely low residual concentrations of electrically active impurities. The concentration of isovalent impurities in all samples was determined by secondary ion mass spectroscopy (SIMS) and in those samples having concentrations of isovalent impurities high enough to produce a significant shift of the band edge, the SIMS results were confirmed by photoluminescence measurements.

The resistivities, listed in Table I, are all high, indicating that added impurities have been incorporated as isovalent centers and that the samples have low concentrations of charged centers. In the unlikely circumstance that the high resistivities of our samples are actually due to compensation, and that the spread of resistivities in the samples is indicative of variations in the degree of compensation (and in the concentration of charged centers) one would expect variations in the NMR line shape which correlate with the variations in resistivity. However, no observable effects on the line shape correlated with resistivity; all of the trends in the quadrupolar broadening observed in these NMR experiments correlated with the level of isovalent doping. In addition, the experiments performed by Rhoderick showed that the grinding procedure alone produced a loss of intensity in the NMR signal which was attributed to strain induced by dislocations. Finally, in a previous study,[13] we found no observable difference between first-order broadening

TABLE I. Properties and growth conditions for GaAs samples used in the NMR studies reported in this paper.

Sample	Dopant	Concentration (cm^{-3})	Resistivity (Ω cm)	Growth conditions
No. 1	In	1×10^{18}	1.1×10^{8}	As rich
No. 2	In	1×10^{18}	4.4×10^{8}	As rich
No. 3	In	1×10^{19}	6.4×10^{7}	Ga rich
No. 4	In	7×10^{19}	4.0×10^{7}	As rich
No. 5	In	2×10^{20}	2.0×10^{5}	As rich
No. 6	Sb	1×10^{19}	5.4×10^{4}	Ga rich
No. 7	Sb	1×10^{19}	2.2×10^{5}	As rich

due to Sb on the As site and In on the Ga site (which we focus on in this work). For these reasons we conclude that the quadrupolar broadening observed in our NMR experiments is attributable to the strain induced by the isovalent impurities and that the effect of charged centers is insignificant.

B. NMR technique

The NMR measurements were carried out at room temperature using pulse spin echo techniques. The pulsed rf system included a Wavetek frequency synthesizer, a Matec model 515 gated amplifier, a Matec model 615 broadband receiver with a tuned preamplifier, and auxiliary equipment operating in a single coil, phase detection mode. Free induction decay curves and spin echo data were signal averaged and then transferred to a computer for fast Fourier transform (FFT) processing to obtain the resonant absorption spectra in the frequency domain.

High intensity static magnetic fields were generated by several superconducting magnets operating between 6 and 13 T. The field was varied to distinguish frequency-dependent (proportional to $1/\nu_0$) second-order quadrupole broadening from the frequency-independent first-order effects and to sharpen the second-order broadened spectral features.

Sample volumes were kept small to limit the effects of field inhomogeneity on the observed line shapes. The 0.7-mm-thick semi-insulating GaAs wafers were cleaved into rectangles and stacked so the single crystal orientation was maintained. A typical sample consisted of a stack of three rectangles with a length of 3 mm and a width of slightly less than 3 mm. The rf transmitter-receiver coil which accommodated these samples was cylindrical, about 5 mm in length with a diameter of 4 mm. The sharp contrast between the widths, spin-lattice, and spin-spin relaxation times of the narrow central portion of the NMR spectra and the very broad first-order quadrupole satellite transitions made it necessary to acquire data using several different pulse sequences in order to obtain accurate representations of all portions of the NMR spectra. A pulse echo technique was used to study the broad central resonance signal. This broad resonance was found to decay in 10–40 μs, a time comparable to the width of the pulse plus the dead time of the receiver (<15 μs). The 90° pulse widths were of the order of 3 μs. This implies that the fields generated (assuming a square pulse) were of the order of 10^{-2} T. Several pulse sequences were used. The results of the various pulse sequences were in substantial agreement with the predictions of Kanert and Mehring for a 90°-β° pulse sequence.[14] An additional pulse sequence of 45°-90° was sued to emphasize the second-order broadened features of the lineshape.[15] The most common pulse sequences used in this study were the 90°-60° sequence and 90°-24° sequence which maximized the total echo for spin-$\frac{3}{2}$ nuclei (^{69}Ga and ^{75}As) and spin-$\frac{9}{2}$ nuclei (^{115}In), respectively. Other useful pulse sequences were the 90°-105° sequence which gives only the satellite transitions and the 90°-180° sequence which gives only the central transition in the echo.

A 90° pulse was judged as the minimum (first) pulse at which a null in the free induction decay (FID) following the second pulse was observed. This condition was not always rigorously obtained but in every case a sharp minimum was obtained. The fact that a null was not obtained is due to some lack of homogeneity in the rf magnetic field but this effect is small. For all of the samples except the most heavily doped one (sample No. 5) the broad portion of the line shape was less than 100 kHz, which is nominally the coverage of a 10^{-2}-T rf field for the ^{75}As nucleus. The Fourier transform was initiated from the nominal maximum of the echo and, with small linear phase corrections, the result was a reasonably symmetric line shape with a flat base line.

Most NMR studies of semiconductors have been carried out on the major constituent nuclear species and relatively few studies of the impurity or dopant atoms have been reported. However, the high sensitivity afforded by the pulse and signal averaging techniques and the Larmor frequencies made accessible by the available magnetic fields make it possible to observe the ^{115}In NMR line in our most heavily doped GaAs samples. One important question to be addressed by the impurity NMR was the possibility of clustering of the In atoms. If the In atoms are clustered or paired, one would expect them to be on sites of reduced symmetry and therefore to experience substantial quadrupolar broadening. On the other hand, if the In atoms are isolated the symmetry of the site should remain tetrahedral although, as we see below, the In atom will induce significant strain fields which distort the symmetry of neighboring lattice sites.

In Fig. 1 the ^{115}In spectra for our most heavily In-doped sample is shown. The spectrum is comprised of two components: a sharp central line with a full width at half maximum (FWHM) of 4.1 kHz and containing about 20% of the intensity, and a broad component, FWHM = 53.6 kHz, containing about 80% of the intensity. The observed intensity ratio corresponds reasonably well to the ratio of satellite to central line intensity (85%:15%) expected for an $I=\frac{9}{2}$ system such as indium.[7] Previous investigations on undoped InAs gave a sharp line (FWHM = 3.1 kHz) with the width primarily due to heterogeneous dipolar interactions with the four nearest-neighbor As nuclei as well as exchange interactions in reasonable agreement with our result.[16]

We attribute the broad component to the first-order quadrupolar effects from overlapping strain fields of In atoms, randomly distributed on the gallium sublattice and assume that the strain at a given In atom is due primarily to the nearest-neighbor In. Using an elastic continuum model the strain at a lattice site due to a point defect gives an electric field gradient

$$V_{zz}=3SS_{11}/(2r^3)f_p \ , \tag{5}$$

where

$$S=\tfrac{1}{3}r_0^2(r_p-r_0)(1+\nu_p)/(1-\nu_p) \ ,$$

with r_0 the GaAs bond length, r_p the InAs bond length, and ν_p, Poisson's ratio of elastic constants. S_{11} is one ele-

ment of the tensor which couples the electric field gradient to the elastic strain (for this work we use the value of S_{11} measured for ^{69}Ga in GaAs and scale it by the ratio of Sternheimer antishielding factors for In and Ga) and f_p is a function of the direction of the magnetic field and the direction vector between In atoms; for simplicity we take the magnetic field to be along the [100] crystallographic direction and f_p reduces to

$$f_p = -[1-(x_i/r_i)^2] , \tag{6}$$

where x_i represents the component of the distance r_i along the [100] direction. To calculate a line shape we take a random distribution of indium atoms and for each find its nearest neighbor and calculate the strain (and electric field gradient) due to it. This gives us a broad line shape with some sharp, angularly dependent, structure superimposed on it. We convolute this line shape with a Lorentzian function which removes the sharp structure and its angular dependence without widening the line appreciably. The Lorentzian function is a simple model of a number of factors, including strain from atoms further away than the nearest neighbor, dipolar effects, and exchange interactions. To remove the sharp structure requires a width of about $(m-\frac{1}{2})$ 10 kHz—that is, 10 kHz for $\frac{1}{2}$ to $\frac{3}{2}$, 20 kHz for $\frac{3}{2}$ to $\frac{5}{2}$, and so forth. Assuming that the dipolar and exchange terms give about 4 kHz, most of the broadening is due to strain from other indium atoms. From our simple calculation we expect the strain from the second-nearest neighbor to be about half of that from the nearest-neighbor indium, in reasonable qualitative agreement with our results. As can be seen in Fig. 1, the broad portion of the line is reasonably well modeled by this simple calculation which, other than the convolution function, has no adjustable parameters. This clearly indicates that the In atoms are not clustered but rather randomly distributed.

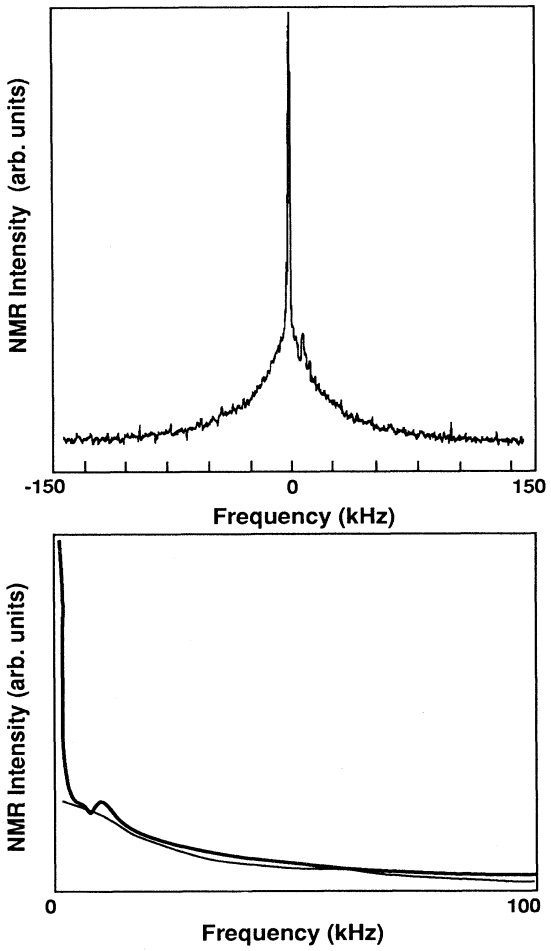

FIG. 1. Top, the ^{115}In NMR spectra of GaAs:In at 41.9 MHz and bottom, the calculated fit (narrow line) to the satellite component of the In NMR data (broad line) shown above.

VI. BOND-ANGLE DISTORTIONS IN THE VICINITY OF In IMPURITY ATOMS: SECOND-ORDER QUADRUPLE INTERACTIONS

The ^{75}As nucleus has a substantial quadrupole moment and also exhibits strong quadrupolar effects if located on a distorted lattice site.[7,14] Furthermore, ^{75}As chemical shifts vary little for As-containing III-V binaries and therefore should not differ appreciably for As atoms at various positions in GaAs:In.[7] In Fig. 2 we show the ^{75}As spectra for two samples with different In concentra-

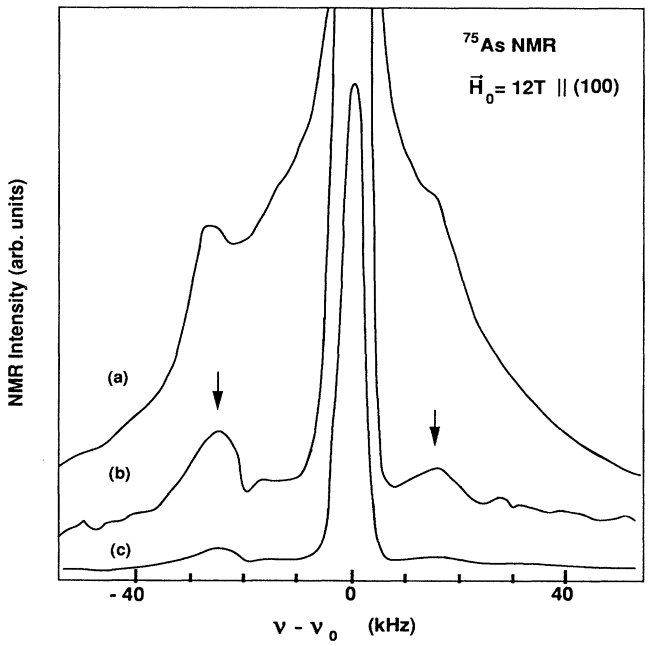

FIG. 2. The ^{75}As NMR spectra of the two samples with the highest indium concentrations (a) 7×10^{19} In/cm^3 and (b) 2×10^{20} In/cm^3. (c) is the spectra in (b) reduced to show the relative intensities of the second-order features, indicated by arrows, and the central line.

tions. The pulse sequence (a 45° pulse followed by a 90° pulse) accentuates the central transition.[14] Of particular interest are the relatively weak features on either side of the strong central resonance.[11] These features are shown to be due to second-order quadrupolar shifts of the central transition by varying the Larmor frequency and observing that the shifts increase with decreasing frequency.

A first consideration is that these features might be due to the four As atoms around the substitutional In atom and it is important to firmly establish that those atoms are not the origins of these features before proceeding. For these four nearest-neighbor arsenic atoms the only distortion which is consistent with the high symmetry of the In atom is a simple trigonal ⟨111⟩ distortion. However, a trigonal distortion is not consistent with the observed dependence of these features on the orientation of the magnetic field. For the particular orientation [100] shown in Fig. 2 only one peak would be observed for a trigonal distortion rather than the two observed. Furthermore, we can readily see [by substituting $\theta=0$ or 109.5° and $\eta=0$ into Eq. (4)] that for H_0 parallel to the ⟨111⟩ direction no second-order shift would be observed for the trigonal distortion, while we detect two peaks.

On the other hand, the next-nearest-neighbor arsenic atoms to the In atom will have reduced symmetry while still retaining one {110} mirror plane. For high-symmetry directions the observed angular dependence is consistent with an EFG having a ⟨110⟩ direction as the principal axis. (In this symmetry argument we neglect the azimuthal dependence.) For H_0 parallel to the [100] direction, an EFG with a ⟨110⟩ principal axis has $\theta=45°$ or 90° and two shifts having a ratio of −7:4 and an intensity ratio of 2:1, respectively, which is approximately our observation. With H_0 parallel to a ⟨111⟩ axis we then expect two peaks of equal intensity on either side of ν_0, with the shift to higher frequency 60 of that to lower frequency, again in agreement with our data.

Having established the principal axis as the ⟨110⟩ by symmetry arguments, the angular dependence is then fit by a quadrupole coupling constant ν_Q of 2.5 MHz and an asymmetry parameter, $\eta=0.2$ (the y axis is another ⟨110⟩). Note that the inclusion of the azimuthal dependence (nonzero η) does not affect the intensity ratios for high-symmetry directions discussed above but does affect the relative shifts. The results of this fit to Eq. (4) are shown in Fig. 3. While we emphasize that the assignment of these features to next-nearest neighbors is based on their orientation dependence, we further note that the intensity of these features is also consistent with this assignment. We compare the intensity of the second-order features with that of the sharp central line which contains almost all of the ($\frac{1}{2}$ to $-\frac{1}{2}$) transitions and very little response due to satellite transitions. Because our intensity arguments are based solely on comparison of the relative intensity in the weak second-order shifted features ($\frac{1}{2}$ to $-\frac{1}{2}$) and the central line ($\frac{1}{2}$ to $-\frac{1}{2}$), the fact that the pulse sequence accentuates the $\frac{1}{2}$ to $-\frac{1}{2}$ transitions relative to the $\frac{3}{2}$ to $\frac{1}{2}$ transitions does not invalidate the intensity comparison. In the case of our most In-rich sample 4% of the As atoms are nearest neighbors to an In atom,

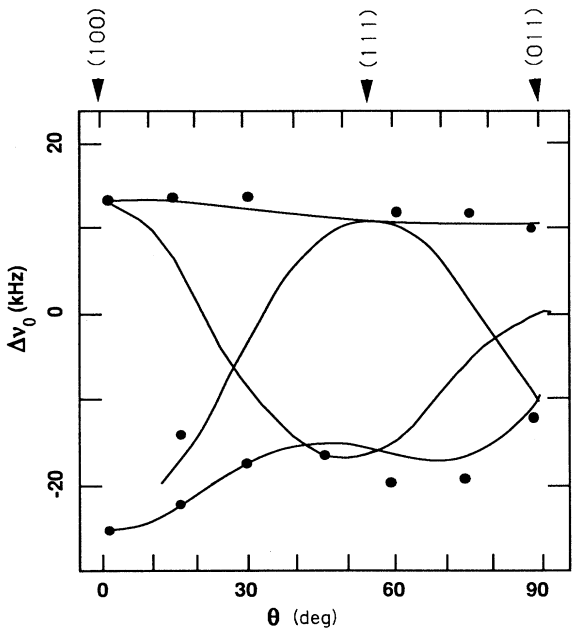

FIG. 3. The angular dependence of the second-order structure shown in Fig. 2. The lines indicate a fit of the second-order shifts to Eq. (4) with $\eta=0.2$ and $\nu_Q=2.5$ MHz.

while 12% are next-nearest neighbors. While it is difficult to make extact intensity measurements due to uncertainties in the base line, we estimate that the intensity in these features is $\geq 10\%$ of that in the central line, a result clearly consistent with an assignment to the next-nearest-neighbor As atoms rather than the nearest neighbors.

Knowing the ν_Q and the asymmetry parameter for the next-nearest-neighbor As atoms, we can estimate the magnitudes of the distortions around those atoms and the distortions around atoms on other shells. The recent EXAFS studies of $Ga_{1-x}In_xAs$ alloys by Mikkelsen and Boyce have shown that the Ga—As and In—As bond lengths vary by less than 2% across the alloy system.[4] They also estimate bond-angle deviations on the order of a few degrees for a 50-50 alloy. Sundfors, Tsui, and Schwab have used nuclear acoustic resonance (NAR) to determine the elements of the tensor which couple EFG to the elastic strain.[8] In this work we use their experimentally determined parameters, S_{ij}, to convert the EFG's into macroscopic strains, ϵ_{ij}, and in turn convert the strains into microscopic bond-angle distortions. In our calculation we consider a cube with the As atom at the center and Ga atoms on four corners as shown in Fig. 4. Two of the Ga atoms are nearest neighbors to the In atom, one is a second-nearest neighbor, and one is a third-nearest neighbor. We assume that the largest bond-angle distortion is at the angle between the two nearest-neighbor Ga atoms and the As atom and for simplicity we treat the other two Ga atoms as equivalents. The principal axes of the EFG tensor are [110], [$1\bar{1}0$],

and [001]; for this calculation we transform that tensor to standard Cartesian coordinates to give

$$\begin{aligned} V_{11} &= \tfrac{1}{4}(1+\eta)V_{zz} = S_{11}[\epsilon_{11} - \tfrac{1}{2}(\epsilon_{22}+\epsilon_{33})] , \\ V_{22} &= \tfrac{1}{4}(1+\eta)V_{zz} = S_{11}[\epsilon_{22} - \tfrac{1}{2}(\epsilon_{11}+\epsilon_{33})] , \\ V_{33} &= -\tfrac{1}{2}(1+\eta)V_{zz} = S_{11}[\epsilon_{33} - \tfrac{1}{2}(\epsilon_{11}+\epsilon_{22})] , \\ V_{12} &= V_{21} = \tfrac{1}{4}(3-\eta)V_{zz} = S_{44}\epsilon_{12} = S_{44}\epsilon_{21} , \end{aligned} \tag{7}$$

and all other terms equal to zero. We can easily show that $\epsilon_{11}=\epsilon_{22}$ and that the strain may be written as the sum of two tensors;

$$\begin{bmatrix} \epsilon_{11} & 0 & 0 \\ 0 & \epsilon_{11} & 0 \\ 0 & 0 & \epsilon_{11} \end{bmatrix} + \begin{bmatrix} 0 & \epsilon_{12} & 0 \\ \epsilon_{12} & 0 & 0 \\ 0 & 0 & \epsilon_{33}-\epsilon_{11} \end{bmatrix} . \tag{8}$$

The first term is a uniform dilation which has no effect on the electric field gradient; the elements of the second strain tensor are then

$$\epsilon_{12} = \tfrac{1}{4}(3-\eta)V_{zz}/S_{44} \tag{9a}$$

and

$$\epsilon_{33}-\epsilon_{11} = -\tfrac{1}{2}(1+\eta)V_{zz}/S_{11} . \tag{9b}$$

From his NAR measurements, Sundfors has determined $S_{11}=0.93\times10^{16}$ dyn$^{1/2}$cm^{-2} and $S_{44}=1.88\times10^{16}$ dyn$^{1/2}$cm^{-2} for ^{75}As in GaAs. We note that these parameters have also been derived from external stress experiments;[17] however, while the NAR and external stress give similar results for rocksalt crystals, the results of the two methods differ significantly for zinc-blende compounds.[8,14] Furthermore, the external stress experiments on zinc-blende crystals give results which differ significantly from compound to compound. For instance, while we would expect similar S_{ij} of ^{75}As in GaAs and InAs, in GaAs (InAs) $S_{11}=2.0\times10^{15}$ (0.8×10^{15}) dyn$^{1/2}$cm^{-2} and $S_{44}=5.8\times10^{15}$ (0.2×10^{15}) dyn$^{1/2}$cm^{-2} for ^{75}As when measured by applying an external stress. The NAR results for ^{75}As in InAs are only a few percent different than those for GaAs.[8] Note that even the ratio S_{11}/S_{44} differs by over an order of magnitude when determined by external stress measurements. For these reasons, we choose to use the strain-EFG coupling parameters determined by the NAR experiments of Sundfors. Using Eq. (9) and our measured EFG we then determine $\epsilon_{12}=0.0147$ and $\epsilon_{33}-\epsilon_{11}=-0.0242$. To convert these strains to bond-angle distortions, we add in a uniform dilation, ϵ_{11}, which allows us to keep the Ga—As bond lengths equal to those in pure GaAs, as indicated by the EXAFS data of Mikkelsen and Boyce. This yields $\epsilon_{11}=-\epsilon_{33}=0.0121$ and $\theta_1=\cos^{-1}[1-\frac{4}{3}(1+\epsilon_{12}+2\epsilon_{11})]=112.7°$ or $\delta\theta_1=3.2°$ and $\theta_2=\cos^{-1}[1-\frac{4}{3}(1-\epsilon_{12}+2\epsilon_{11})]=110.2°$ or $\delta\theta_2=0.7°$. From our measured value of θ_1 we then calculate a value of 107.5° for the angle between the In atom, the nearest-neighbor As atom, and the nearest-neighbor Ga atom if we assume that the In—As bond length is 2.585 Å—the value which Mikkelsen and Boyce obtain for the InAs bond length in GaAs-rich GaAs:InAs alloys.[4] The EFG should be roughly proportional to the difference between the bond angle and 109.5° and, since the structures observed are second order, the shifts from the center of the spectra should scale as the deviations in bond angle squared. From this simple argument, we would expect the second-order quadrupolar shifts of the four nearest-neighbor As atoms to be about 40% of those of the 12 next-nearest neighbors. In our current measurements the combination of weaker intensity due to a third as many As atoms and the smaller shift away from the strong central line could render the signature of the nearest neighbors unobservable. Furthermore, if the S_{ij} are actually somewhat smaller and those determined from NAR measurements, the bond-angle distortions around the next-nearest-neighbor As atoms would in turn be larger and those around the nearest neighbor would be smaller which would certainly leave the structure due to the nearest neighbors under the central line. Finally we calculate the angle between the nearest-neighbor As, the nearest-neighbor Ga, and the next-nearest-neighbor As (θ_3 in Fig. 4) to be 109.6°, which explains why no second-order structure is observed in the ^{69}Ga spectra. This is very consistent with the EXAFS data which indicate that As-As distance depends

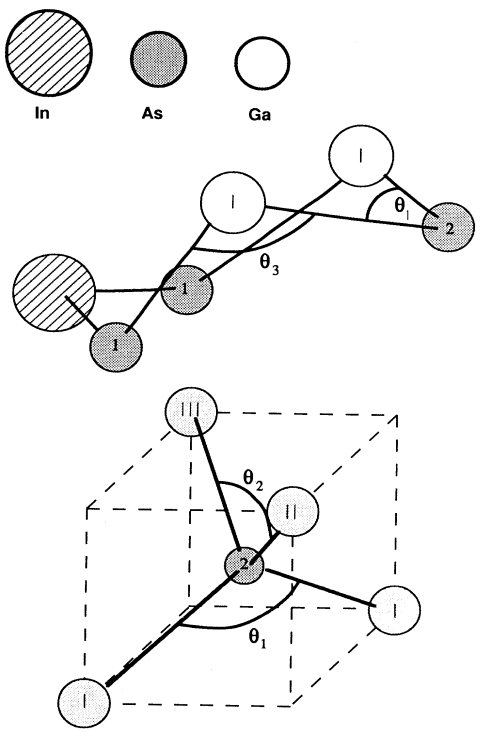

FIG. 4. The relative positions of the first shells of As and Ga atoms to each other in a basic tetrahedron and a six member ring which includes the three atomic species in GaAs:In. The specific bond angles discussed in the text are also shown.

only on the intervening cation.[4] Therefore, since the Ga-As distances and the As-As distancs are the same as those in GaAs, the angle should also be tetrahedral.

VII. SPATIAL EXTENT OF THE STRAIN FIELD: FIRST-ORDER QUADRUPOLAR INTERACTIONS

The ^{75}As NMR spectra for four GaAs samples with In concentrations ranging from 2×10^{18} to 2×10^{20} cm^{-3} are shown in Fig. 5. These spectra were obtained using a 90°-60° pulse sequence which gives equal weight to the central and satellite transitions and should therefore closely approximate a cw NMR spectrum. In these spectra the second-order features due to the next-nearest-neighbor As atoms are not so obvious, but the first-order satellite transitions are observed as wings or shoulders in the case of dilute or concentrated samples, respectively. The shapes or widths of these broad wings or shoulders are independent of the Larmor frequency and crystal orientation relative to the magnetic field, indicating that they are produced by first-order interactions and that they are qualitatively similar to powder patterns and the In spectra discussed in Sec. V. The line shape can be understood on the following basis. Each As atom on a relatively distant coordination sphere surrounding an isolated impurity atom will experience a strain of identical magnitude which is a decreasing function of the radius r of the coordination sphere. The quadrupole interaction is also a function of the angle between the principal axis of the EFG tensor and the applied magnetic field. The line shape here is qualitatively similar to that observed for the indium nuclei; however, the details of the analysis are somewhat different. In the case of the indium nuclei both the source of the strain field and the resonating nucleus are on the same sublattice and the question of how the strain was distributed between the two sublattices never entered the analysis; i.e., the scale of distances in Eq. (5) was simply the bond length. In the case of the arsenic resonance, where the center of the strain field and the resonating nucleus are on opposite sublattices, the distribution of strains between the cation and anion sublattices is an additional parameter. The length scale (and, hence, the frequency scale) is not established *a priori*, as it was in the case of the indium NMR.

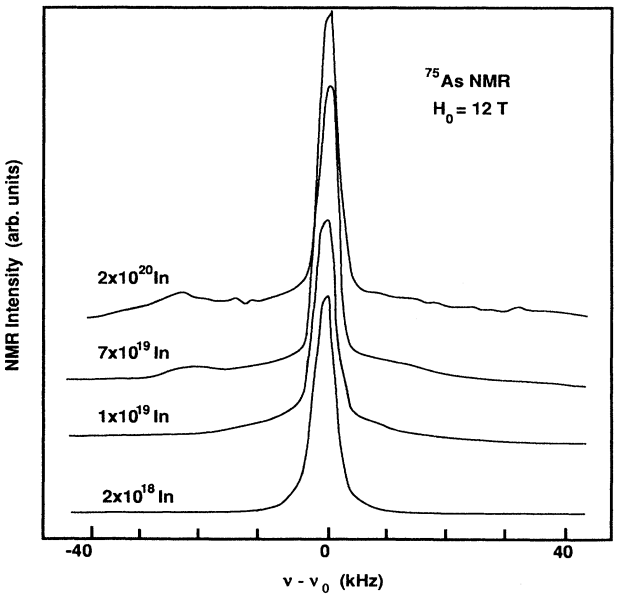

FIG. 5. The ^{75}As NMR spectra of GaAs:In having various indium concentrations as indicated in the figure.

The smallest coupling constant observable is that for which the first-order splitting of the satellite transitions just exceeds the width of the central resonance (1.5 kHz).[7] Thus that portion of the wings or shoulders just outside the central resonance is contributed by the most distant atoms for which the distortion is sufficient to produce an observable quadrupole interaction. (For the present purposes we define the separation of these atoms from the impurity as the spatial extent of the strain field.) Conversely, the largest observable coupling constant is determined by the splitting or shift for which the diminishing tails of the first-order wings are just distinguishable from the noise. As reported in Sec. VI, the quadrupole coupling constant for the next-nearest-neighbor As atoms, measured from the NMR spectra of Fig. 2 is 2.5 MHz. Knowing the quadrupole coupling constant for the next-nearest-neighbor As atoms, which constitute the second coordination sphere of the As atoms surrounding an In impurity, one can use the isotropic continuum approximation[18] (which assumes that the strain and the quadrupole coupling constant drop off as r^{-3}) to calculate the coupling constants for all of the As coordination spheres. This r^{-3} distribution of coupling constants can then be used to simulate the first-order satellite line shape for the ^{75}As NMR spectra. The line shape of the first-order wings has been simulated by calculating the expected coupling constant for each As coordination sphere on the r^{-3} model (assigning a value of 2.5 MHz for the second coordination sphere) and weighting the powder pattern intensity for each of these coupling constants according to the number of As atoms on each coordination sphere as calculated for the zinc-blende lattice. [It can be shown analytically that the line shape generated by such a numerical simulation corresponds to satellite intensity distributions which are proportional to $\Delta\nu_0^{-2}$ where $\Delta\nu_0$ is the frequency shift from the Larmor frequency ($\Delta\nu_0=\nu_0-\nu$).]

The $\Delta\nu_0^{-2}$ line shape is compared to the experimentally observed ^{75}As NMR line shape for samples with three different In dopant concentrations in Fig. 6. It is evident that the line shape for In concentrations of 1×10^{19} cm^{-3} or lower are well fitted by this approximation. It is possible to determine from the simulation that the smallest observable first-order interaction, i.e., where the first-order satellite wing just merges with the central line, corresponds (in the r^{-3} model) to the 50th coordination sphere of the As sublattice (radius of 28 Å). Thus simulation of the first-order line shape indicates that the effects of the

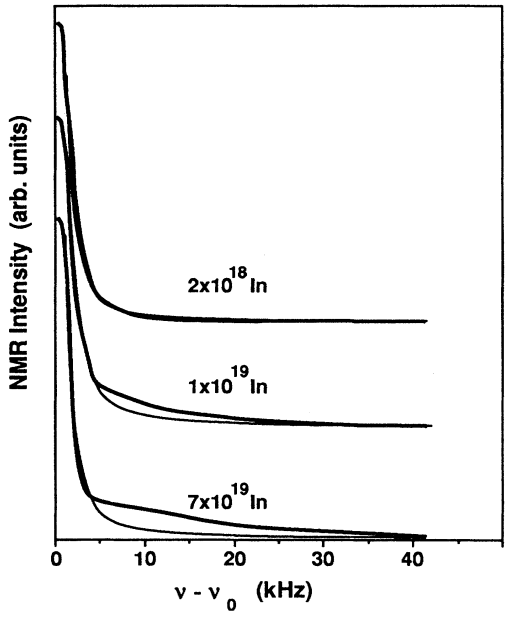

FIG. 6. A fit (narrow line) of the first-order wings to a $\Delta\nu_0^{-2}$ dependence. Note that for high concentrations the wings deviate near $\Delta\nu_0=0$ due to atoms relatively far from an In atom and therefore more affected by overlapping strain fields.

strain introduced by an isolated In impurity atom are observable as a quadrupolar perturbation of the ^{75}As NMR spectrum at distances up to 28 Å from the In atom.

An independent estimate or confirmation of the extent of the strain field can be inferred from the expectation that these 56-Å-diam spheres should just begin to have significant overlap at a concentration of 1×10^{19} cm^{-3} (In-In separation of 46 Å). As expected under this working hypothesis, the r^{-3} or $\Delta\nu_0^{-2}$ line shape fits spectra for all samples with In concentrations below this level. However, at higher concentrations substantial overlap of spheres of induced strain occurs (In-In separation of 24 Å for 7×10^{19} cm^{-3}) and the first-order line shape develops distinct shoulders indicating that the strain at distant As atoms does not drop below some minimum value because of the effects of overlapping strain fields (see Figs. 5 and 6).

It should be emphasized that the fact that we have fitted the assumed r^{-3} curve for the spatial dependence of the quadrupole coupling constant to the 2.5-MHz value measured for the next-nearest-neighbor As atoms does not mean that we believe that the strain follows an r^{-3} power law exactly to such short range. Our justification for making this assumption in our working hypothesis is that for distant atoms which contribute to the observed satellite wings the procedure works well for In concentrations less than 1×10^{19} cm^{-3} (i.e., concentrations for which the In atoms can be treated as isolated impurities with little overlap in their strain fields). Another independent confirmation of the estimated spatial extent of the strain field is provided by the dependence of the relative intensities of the central resonance and the first-order wings upon In concentration. If the radius of the sphere of influence estimated from the line shape is correct, then at a concentration of 1×10^{19} cm^{-3} the overlapping strain fields are just sufficient to remove all first-order satellite intensity from the narrow central resonance. That is, every As site in the crystal will experience a distortion at least large enough to split out its first-order satellite transitions. (Note that 40% of the intensity is contained in the $m=\frac{1}{2}$ to $-\frac{1}{2}$ transitions and 60% in the satellite transitions for a spin-$\frac{3}{2}$ nucleus.) Therefore the intensity of the central resonance divided by 0.4 should approximately equal the total intensity. Our total observed intensity for the sample having an In concentration of 1×10^{19} is only about 90% of that which is expected on this basis. The missing 10% of the intensity is explained as follows. The largest observable first-order quadrupole interaction (maximum width of the satellite wings) corresponds to atoms on the 12th coordination sphere of the As sublattice. All As atoms with in this sphere (i.e., closer to the In atom) have too broad a first-order satellite line to be observable. The 12th coordination sphere encloses a total of 240 As atoms (for each In impurity atom) which for an In concentration of 1×10^{19} cm^{-3} corresponds to about 10% of the As atoms, consistent with the magnitude of the missing NMR intensity. The arguments based upon the intensities of the satellite transitions are consistent with the results of Rhoderick, who has reported cw NMR derivative spectroscopy of samples of crystalline GaAs:In. He measured the intensity of the observed central ^{69}Ga resonance as a function of In concentration and found that it was reduced to 40% of its value in undoped GaAs at concentrations between 1×10^{19} and 1×10^{20} cm^{-3}.

VIII. CONCLUSIONS

In summary, we have demonstrated that the In atoms in GaAs:In are randomly distributed at substitutional sites and suggested that the same may be true for other isovalent impurities. By observing the strain-induced quadrupolar interactions between neighboring In atoms we are able to determine an average separation and therefore conclude that the In atoms are randomly distributed. By measuring the ^{75}As NMR we are able to examine the distribution of strain in the lattice and find that the strain induced by these substitutional impurities is observable over distances of about 30 Å. Using a result from NAR experiments which give the relationships between strain and electric field gradients at the nuclear sites we can use our observed second-order quadrupolar shifts in the ^{75}As NMR spectra to deduce the bond-angle distortions for the next-nearest-neighbor shell of As atoms around the substitutional In atom. From this we derive bond-angle distortions around the first shells of Ga and As atoms. The results give significantly smaller bond-angle distortions for both near-neighbor shells which is consistent with our own null results and with previous EXAFS results for more concentrated alloys which indicated that the As-As distances should be unperturbed.

ACKNOWLEDGMENTS

The authors gratefully acknowledge W. Mitchell (Materials Laboratory, Wright-Patterson Air Force Base) and R. N. Thomas (Westinghouse Research and Development Center) for providing the samples used in this study. We also wish to thank Z. M. Saleh and P. C. Taylor of the University of Utah who graciously provided the indium spectra used in this work. The cooperation of R. J. Wagner and the staff of the Naval Research Laboratory High Magnetic Field Facility is greatly appreciated.

---

*Present address: Center for Compound Semiconductor Microelectronics, University of Illinois at Urbana-Champaign, Urbana, IL 61801.

[1]M. G. Mil'vidsky, V. B. Osvensky, and S. S. Shifrin, J. Cryst. Growth **52**, 396 (1981).

[2]G. Jacob, M. Duseaux, J. P. Farges, M. M. B. Van der Boom, and P. J. Roksnoer, J. Cryst. Growth **61**, 471 (1983).

[3]H. M. Hobgood, R. N. Thomas, D. L. Barrett, G. W. Eldridge, M. M. Sopira, and M. C. Driber, in *Semi-insulating III-V Materials,* edited by D. C. Look and J. S. Blakemore (Shiva, Nantwich, U.K., 1984), p. 149.

[4]J. C. Mikkelsen and J. B. Boyce, Phys. Rev. B **28**, 7130 (1983).

[5]Katsuhiro Akimoto, Yoshifumi Mori, and Chiaki Kojima, Phys. Rev. B **35**, 3799 (1987).

[6]Kebede Beshah, David Zamir, Piotr Becla, Peter A. Wolff, and Robert G. Griffin, Phys. Rev. B **36**, 6420 (1987).

[7]R. L. Mieher, in *Semiconductors and Semimetals,* edited by R. K. Willardson and A. G. Beer (Academic, New York, 1966), Vol. 2, Chap. 7.

[8]R. K. Sundfors, Phys. Rev. B **20**, 3562 (1979); R. K. Sundfors, R. K. Tsui, and C. Schwab, *ibid.* **13**, 4504 (1975).

[9]M. K. Cueman, R. K. Hester, A. Sher, and J. F. Soest, Phys. Rev. B **12**, 3610 (1975).

[10]E. H. Rhoderick, J. Phys. Chem. Solids **8**, 498 (1958).

[11]W. E. Carlos, S. G. Bishop, and D. J. Treacy, Appl. Phys. Lett. **49**, 528 (1986).

[12]M. Cohen and F. Reif, in *Solid State Physics: Advances in Research and Applications,* edited by F. Seitz and D. Turnbull (Academic, New York, 1957), Vol. 5, p. 321.

[13]W. E. Carlos, S. G. Bishop, and D. J. Treacy, in *18th International Conference on the Physics of Semiconductors, Stockholm, 1986,* edited by O. Engström (World Scientific, Singapore, 1987), p. 947.

[14]O. Kanert and M. Mehring, *Static Quadrupole Effects in Disordered Cubic Solids, NMR—Basic Principles and Progress* (Springer, Heidelberg, 1971), Vol. III.

[15]In this paper we define a 90° pulse as one which maximizes the free induction decay if all transitions are considered.

[16]R. G. Shulman, J. M. Mays, and D. W. McCall, Phys. Rev. **100**, 692 (1955); R. G. Shulman, B. J. Wyluda, and H. J. Hrostowski, Phys. Rev. **109**, 808 (1958).

[17]K. A. Dumas, J. F. Soest, A. Sher, and E. M. Swiggard, Phys. Rev. B **20**, 4406 (1979).

[18]J. D. Eshelby, in *Solid State Physics: Advances in Research and Applications,* edited by F. Seitz and D. Turnbull (Academic, New York, 1956), Vol. 3, p. 78.